A Framework for Synthesizing the Optimal Separation Process of Azeotropic Mixtures

Xiao Yang, Hong-Guang Dong*

School of Chemical Engineering, Dalian University of Technology,
Dalian, 116012, PRC

Ignacio E. Grossmann*

Department of Chemical Engineering, Carnegie Mellon University,
Pittsburgh, 15213, USA

ABSTRACT

In this work a systematic framework is introduced to synthesize the optimal separation process of azeotropic mixtures. The proposed framework, which can handle an arbitrary number of components, consists of two main steps: a system analysis and a state-space superstructure algorithm. The system analysis is composed of some equation-oriented algorithms to supply basic information for the superstructure, including structure of the composition space, existence of *unchangeable points* and candidate operations. It is shown that the proposed superstructure featuring multi-stream mixing is superior to previous ones because it significantly expands the feasible area. Moreover, detailed design parameters such as number of stages and reflux ratio are derived. Additionally, flowsheet feasibility test rules are constructed to facilitate the analysis of the process, and are able to be used as heuristic methods to guide the design of ternary or quaternary systems. Two industrial cases are presented to illustrate the proposed framework.

Keywords: process design; state-space superstructure; azeotropic distillation; extractive distillation

*To whom correspondence should be addressed. E-mail: hgdong@dlut.edu.cn (H.G. Dong); grossmann@cmu.edu (I.E. Grossmann)

Introduction

Separation of azeotropic mixtures is common in the chemical industry, but its optimal flowsheet design still faces many challenges. Unlike ideal systems, the first issue with azeotropic mixtures is separation feasibility. Products of columns are restricted within so-called distillation regions[1] and compartments[2, 3]. With the help of useful geometric tools such as residue curve maps (RCMs), considerable research work has been done for testing the feasibility of columns. Besides the pioneering work presented in a series of articles by Doherty and his co-workers, other researchers have also made notable contributions. Fien and Liu[4], and Widagdo and Seider[5]'s excellent reviews cover this research area up to 1994 and 1996, respectively. Works during this period have mainly focused on ternary or quaternary systems, since they are easily visualized. After Fidkowski et al.[6] developed a homotopy-based method for locating all azeotropes, Rooks et al.[7] proposed an equation-based approach for determining distillation region structures of multicomponent homogeneous mixtures using the adjacency and reachability matrix. The work of Rooks et al. makes it quite convenient for studying azeotropic systems with more than four components. More recently, Thong et al.[3] extended the analysis of column feasibility to multicomponent systems using a manifold method.

On the basis of the knowledge of separation feasibility, column sequencing problems have attracted the attention of a number of researches. Doherty and his co-workers used RCMs to study the sequencing problem, first for homogeneous azeotropic distillation[8] and then for heterogeneous azeotropic distillation[9]. Later, Safrit and

Westerberg[10] studied the separation sequence synthesis for batch azeotropic distillation process; Thong et al.[11, 12] developed a systematic procedure to synthesize column sequences for multicomponent homogeneous systems based on their previous work[3] of column feasibility and a set of recycle rules. Actually, a key problem of azeotropic distillation process synthesis is how to deal with recycle streams. Selecting proper recycle streams significantly improves the flowsheet performance, both in terms of purity and recovery. Tao et al.[13] proposed some rules to generate process alternatives with recycle streams. Later, Liu et al.[14] further studied the performance of recycle streams in different types of splits. The above approaches are mainly based on heuristic rules. Mathematical and algorithmic methods have also been applied[15-19]. However, most of these approaches are limited to three component homogeneous systems[15-18]. Bauer et al.[15-17] searches the optimal scheme from a superstructure consisting of a sequence of preferred separations. However, this methodology results in a very large number of constraints for the prospective schemes. Ismail et al.[18] utilized a generalized modular framework to simultaneously solve for the entrainer selection and the column sequencing problem. However, the number of modules has to be determined using a trial-and-error procedure, since columns and their interconnection are not pre-postulated. Yeomans et al.[19] developed a generalized disjunctive programming (GDP) model based on the STN superstructure of Sargent[20] for the optimal design of thermally coupled distillation, which is capable of being applied to azeotropic systems, but their model lacks the flexibility of the location of intermediate streams motivated by mixing and splitting. Feng et al.[21] proposed an algorithm for synthesizing an

azeotropic distillation system based on their previous work[22] of partitioning the composition space and then identifying candidate operating units. However, their method leads to processes that lack flexibility of multi-stream mixing and splitting of streams for different operation units. Moreover, although the authors claimed their method is applicable to multicomponent systems, it is difficult to derive an automated workflow. In fact, as the number of components increases, it is laborious to identify candidate operations. Finally, since their objective function is rather simplified, it lacks a proper evaluation method to assess the flowsheet.

In this work, a systematic framework is constructed for the flowsheet synthesis for separation process of azeotropic mixtures. The proposed framework is applicable to both homogeneous and heterogeneous systems with arbitrary number of components. The core of the framework is a state-space superstructure algorithm, which has been first proposed by Bagajewicz et al.[23, 24] as a representation of mass and heat exchange network. In this article, a modified superstructure is developed to represent separation network of azeotropic mixtures. In addition, a system analysis made up of several equation based algorithms is used for supplying basic information for constructing the superstructure with the given system.

Perfect Recovery

Due to the existence of distillation boundaries, high purities and high recoveries of certain components are usually difficult to obtain in the separation of azeotropic mixtures. Either high purity is obtained with poor recovery, or high recovery is obtained with low purity. For azeotropic distillation, mixing with recycle streams is the

most basic way to improve separation performance, but it is not always effective. Hence, at the beginning of the flowsheet design task, it is necessary to identify which species are able to be separated with both high purity and high recovery by distillation and mixing, and which ones are not. After that, proper auxiliary methods are introduced to facilitate the separation. In this work, a method that applies to the entire flowsheet is developed for detecting the limitation of azeotropic distillation.

If all the species are able to be separated with both high purities and high recoveries, we denote it *perfect recovery*. Later we show that attaining perfect recovery depends on the topological structure of the mixture's RCMs, starting from the following *mixing-distillation pair and separation validity lemma*.

Mixing-Distillation Pair and Separation Validity Lemma

First, for a concise formulation of the overall model, assume that

(1) Any distillation is performed in simple columns, with one feed and two products.

(2) Distillation boundaries are linear, so no distillation boundary crossing separation is considered.

Vogelpohl[25] showed that azeotropes behave like pure components and consequently a distillation region or compartment is equivalent to a hypothetical ideal system composed of its vertex singular points. Consider a system of A, B and C (see Figure 1(a)), where the entire composition space is divided into three compartments□,□ and □. A stream e located at point P in compartment □ is represented in terms of molar flow of its vertex singular points X, C and A, i.e., $e(fx_e, fc_e, fa_e)$.

Another stream u located at the azeotrope X is produced by some column in the flowsheet and requires further rectification. Similar to e, u is represented as $u(fx_u, 0, 0)$. First mix u with e, then use two sharp separations in sequence to separate the mixture into three products $v1(fx_{v1}, 0, 0)$ located on azeotrope X, $v2(0, fc_{v2}, 0)$ located on the pure component point C and $v3(0, 0, fa_{v3})$ located on the pure component point A (see Figure 1(b)). The sequence of the two separations is not important here, because the final products will be the same. According to mass balance of the overall flowsheet:

$$fx_e + fx_u = fx_{v1} \quad (1)$$

$$fc_e = fc_{v2} \quad (2)$$

$$fa_e = fa_{v3} \quad (3)$$

From the above equations, it is seen that $v2$ of the pure component C is totally supplied by e, which means that u is not further separated, i.e., mixing with e in region □ does not facilitate further rectification of u. In other words, mixing with any stream in the same compartment of the azeotrope stream does not facilitate the azeotropic distillation. This is the so-called *mixing-distillation pair validity lemma*, which reflects the natural behavior of linear distillation boundaries quantitatively.

Unchangeable Point and Perfect Recovery Rule

In a similar way, mixing with any point in compartment □ or □ also does not facilitate further separation of u, which means u has reached the limit of azeotropic distillation. Since u is located at azeotrope X, we call X an *unchangeable point*.

Let us consider the other azeotrope Y in this RCMs. According to the mixing-distillation pair validity lemma, we know that mixing with any stream located in compartment □ or □ will not facilitate further separation of the stream u' located at Y. However, mixing with stream e located in compartment □ is helpful. With a proper flowrate of e, the mixture of u' and e will be placed in compartment □. Since the column feed is located in compartment □, u' is represented in terms of the molar flow of compartment□'s vertex singular points, i.e., $u'(fx_{u'}, fc_{u'}, fa_{u'})$. Obviously, $fc_{u'}$ is negative, i.e., $fc_{u'} < 0$. Also, we use two sequential sharp separations to separate the mixture into three products $v1'(fx_{v1'}, 0, 0)$ located on azeotrope X, $v2'(0, fc_{v2'}, 0)$ located on the pure component point C and $v3'(0, 0, fa_{v3'})$ located on the pure component point A (see Figure 1(c)). Applying the constraints of mass balance:

$$fx_e + fx_{u'} = fx_{v1'} \quad (4)$$

$$fc_e + fc_{u'} = fc_{v2'} \quad (5)$$

$$fa_e + fa_{u'} = fa_{v3'} \quad (6)$$

It is seen from these equations that component A of u' is removed by sacrificing part of component C of e. This part of e leads to an increase of the stream located at azeotrope X.

For any near sharp separation, the two column products are either pure components or streams located on distillation boundaries, compartment boundaries or composition boundaries. Therefore, whether these boundary streams are capable of further rectification decides the recovery levels. Boundary streams are represented in terms of

their vertex singular points so that feasibility of perfect recoveries is based on the topological property of these vertex singular points.

If a point corresponds to the intersection of all compartments, it is called an *unchangeable point*, e.g., X in Figure 1(a). On the other hand, if a point is not the intersection of all compartments, it is called a *changeable point*. Streams located at unchangeable points are not able be further separated without other auxiliary methods such as decanting, extractive distillation, membrane-aided distillation, and pressure-swing distillation. However, streams located at changeable points are able to be further separated by sacrificing some component of the entrainer, and finally are transformed into streams located at unchangeable points. Hence, unchangeable points cause infeasibility of a perfect recovery flowsheet of azeotropic distillation, and therefore, the perfect recovery rule is stated as follows:

Flowsheet feasibility test rule 1: perfect recovery rule

For a separation process involving only mixing and azeotropic distillation, perfect recoveries should involve no unchangeable points in the RCMs.

Unfortunately, according to Serafimov[26]'s classification of topological structures for ternary azeotropic systems, unchangeable points exist in almost all topological structures.

The Proposed Framework

In order to synthesize the optimal separation process of azeotropic mixtures, a

systematic framework is proposed in this work. The framework consists of the following three steps.

1. Apply a system analysis to explore the composition space structure, i.e., compartments and liquid-liquid phase regions, to identify unchangeable points and to define candidate operations.
2. For each unchangeable point, select proper auxiliary methods. In this article, we use decanting to facilitate the separation in a heterogeneous system, and extractive distillation for a homogeneous system. In this step, several candidate entrainers for extractive distillation are selected and the best one is decided in the next step.
3. Use the state-space superstructure algorithm to find the optimal flowsheet. The overall optimization problem is formulated as a mixed-integer nonlinear programming (MINLP) model.

System Analysis

As mentioned in the previous section, the system analysis involves three basic tasks:

(1) Explore structure of the composition space

(2) Identify unchangeable points

(3) Define candidate operations

For a three or four component system, these items are also able to be implemented with conventional geometric methods. But for multicomponent systems, the following equation-oriented method is more efficient.

Explore composition space structure

For azeotropic mixtures, distillation boundaries make it rather difficult to assess the feasibility of a proposed separation. In different regions of the composition space, the potential products of feasible separations are different. Before defining candidate operations, it is necessary to explore the structure of the entire composition space, i.e., identify all distillation regions and compartments, and additional homogeneous and heterogeneous regions for a system with liquid-liquid envelopes. The algorithm for identifying distillation regions and compartments that is mainly based on the work of Rooks et al.[7] and Thong et al.[3], is summarized as follows:

Algorithm 1: identify distillation regions and compartments

1. For the given azeotropic mixture system, specify the pressure and choose a VLE model. Identify all azeotropes and determine their stability using the method proposed by Fidkowski et al.[6]
2. Apply the algorithm proposed by Rooks et al.[7] to generate the directed adjacency matrix and its related reachability matrix, and then identify all distillation regions.
3. For each distillation region, use the algorithm proposed by Thong et al.[3] to search for all compartments.

If there is a liquid-liquid envelope, homogeneous and heterogeneous regions also need to be identified. The procedure proposed in this work is implemented with the following algorithm:

Algorithm 2: identify homogeneous and heterogeneous regions

1. For a given compartment identified by Algorithm 1, write the equation of the liquid-liquid envelope skeleton points in the compartment:

$$LL(\boldsymbol{c}) = 0 \qquad (7)$$

$$\boldsymbol{c} = (c_1, c_2, \cdots, c_M)^T \qquad (8)$$

2. For other points in the compartment, e.g., P and Q, if $LL(\boldsymbol{c}_P)$ and $LL(\boldsymbol{c}_Q)$ have the same sign, then P and Q are in the same region; otherwise they are in the different regions.

3. Distinguish homogeneous and heterogeneous region:

   In one of the two identified regions, for a point P which is not the liquid-liquid envelope skeleton point ske, if:

$$\boldsymbol{c}_P = \sum_{ske \in SKE} \lambda_{ske} \boldsymbol{c}_{ske} \qquad (9)$$

$$\sum_{ske \in SKE} \lambda_{ske} = 1 \qquad (10)$$

$$\lambda_{ske} \geq 0 \quad \forall ske \in SKE \qquad (11)$$

   then the region with P is a heterogeneous region; otherwise, it is a homogeneous region.

4. Repeat step 1-3 for any other compartment.

Identify unchangeable points

It has been demonstrated in section 2 that the existence of unchangeable points is of great importance in azeotropic distillation flowsheet. Before developing the process

optimization model, identifying unchangeable points is helpful to make a judgment of the limitation of azeotropic distillation and then select effective auxiliary methods. From the definition of unchangeable points, a direct geometric method is developed to identify unchangeable points by finding the intersection of all the compartments. But for multicomponent systems, a matrix-oriented method is much more convenient. A generalization of the geometric method is described as follows:

Algorithm 3: indentify unchangeable points

1. According to the result of Algorithm 1, generate the incidence matrix $\boldsymbol{I}$. Every row of $\boldsymbol{I}$ denotes a compartment, and every column of $\boldsymbol{I}$ denotes an azeotrope ranked in the order of boiling temperature. If an azeotrope is the vertex of the compartment, then the corresponding element of $\boldsymbol{I}$ is set to 1, otherwise it is set to 0.
2. For each column, if all elements of the column are 1, then the corresponding azeotrope is an unchangeable point; otherwise it is a changeable point.

For the system shown in Figure 1(a), the incidence matrix is written as follows:

$$\boldsymbol{I} = \begin{array}{c} \\ ¢ \\ ¢ \\ ¢ \end{array} \begin{array}{c} \begin{array}{cc} X & Y \end{array} \\ \begin{bmatrix} ñ1 & 0 \\ ò1 & 1 \\ ó1 & 1 \end{bmatrix} \end{array}$$

Therefore, X is an unchangeable point, and Y is a changeable point. For an element whose value is 0, streams located in its corresponding compartment are used to change the composition of its corresponding changeable point, for example, *e* in

compartment □ helps to remove composition A of u'.

Define candidate operations

Based on the results of the former steps, feasible separations of each compartment are defined in this step. In this work, for simplicity of the model and to reduce computational complexity with process optimization, we consider only sharp separations in simple columns between adjacent components. For a system of more than four components, quite a few of such separations exist and many of them are superfluous. Some rules are embedded in this step to screen out superfluous separations by considering the relationship among compartments. The basic idea is to avoid the repetition of separations of the same species. In other words, separations between a pure component and a changeable point which contains it are undesired. These candidate operations are generated by the following algorithm:

Algorithm 4: define candidate operations

1. Select a compartment, and then define its augmented incidence matrix $\boldsymbol{I'}$. Compared with the incidence matrix $\boldsymbol{I}$, its columns include additional pure component points.
2. For homogeneous systems, check the corresponding column of each pure component point. If there is only one non-zero element in the column, then the pure component is removed from this compartment. Otherwise, eliminate the row containing the changeable point with the pure component, until there is no such

row or there is only one non-zero element left; then the pure component is removed from the compartment corresponding to the remaining rows. The corresponding row of the changeable point at which the composition of the pure component is greater has priority to be eliminated. For heterogeneous systems, no row is eliminated, since the unchangeable point is possible to be broken in the whole heterogeneous region.

3. For homogeneous systems, eliminate rows containing changeable points sharing components with the unchangeable point. For the left rows, if there is an adjacent pure component removed, the unchangeable point is also removed in the corresponding compartment.
4. Repeat Steps 1-3 for all the other compartments.
5. For each compartment, generate separation sequences for the selected singular points which need to be removed in the compartment as illustrated in Figure 2, with the gray and black point representing pure components or unchangeable points and white points representing other azeotropes. By treating each singular point as a pseudo component in an ideal system, the column sequence problem inside a compartment is the same as the conventional sharp split distillation synthesis, and is presented by several binary trees.

For the system shown in Figure 1(a), the incidence matrix is written as follows:

$$\boldsymbol{I}' = \begin{array}{c} \\ \text{¢} \\ \text{¢} \\ \text{¢} \end{array} \begin{array}{c} \begin{array}{ccccc} \text{X} & \text{Y} & \text{C} & \text{B} & \text{A} \end{array} \\ \begin{bmatrix} 1 & 0 & 1 & 0 & 1 \\ 1 & 1 & 0 & 0 & 1 \\ 1 & 1 & 0 & 1 & 0 \end{bmatrix} \end{array}$$

In this system, A is removed in compartment □, not in compartment □, for the

unchangeable point Y in compartment □ contains A. B is removed in compartment □, and C is removed in compartment □. The unchangeable point X is removed in compartment □.

Superstructure

With the information supplied by the system analysis, a state-space superstructure is constructed for the separation network design of azeotropic mixtures (see Figure 3). The superstructure consists of three interconnected blocks, a distribution network (DN), an RCM operator (OP-RCM) and an auxiliary operation operator (OP-AO). Inside the DN, a series of mixers and splitters are placed with connections among all of them. Mixers and splitters are both ranked by the average temperature of their corresponding vertex singular points. Candidate operations generated by the system analysis are configured in OP-RCM, whereas the selected auxiliary operations are arranged in OP-AO. If decanting is selected for facilitating the separation, a series of decanters appear in OP-AO, whereas if extractive distillation is chosen, a series of extractive distillation columns are then embedded. The specific information of each block is described in the next section.

Mathematical Model

Distribution network

Every stream in the flowsheet has two basic attributes, one is flowrate and the other is composition. To specify a stream, we attach it with an operation unit. Specifically, $f_{unit}^{in\ or\ out}$ denotes the flowrate of input or output stream of $unit$, while the vector

$\boldsymbol{c}_{unit}^{in\ or\ out}$, i.e., $\left(c_{unit}^{in\ or\ out,1}, c_{unit}^{in\ or\ out,2}, \cdots, c_{unit}^{in\ or\ out,i}, \cdots, c_{unit}^{in\ or\ out,M}\right)^T$, denotes the composition of the stream. Due to the normalization constraint $\sum_{i=1}^{M} c_{unit}^{in\ or\ out,i} = 1$, the composition of a stream is mapped into a point in an (M-1)-dimensional rectangular coordinate system, represented using a reduced vector $\hat{\boldsymbol{c}}_{unit}^{in\ or\ out}\left(c_{unit}^{in\ or\ out,1}, c_{unit}^{in\ or\ out,2}, \cdots, c_{unit}^{in\ or\ out,i}, \cdots, c_{unit}^{in\ or\ out,M-1}\right)^T$.

In a typical azeotropic distillation process, impure products of columns are recycled and mixed with other streams for further separation. If the stream is not located at an unchangeable point, the recycle improves the process performance. The main task of the DN is to provide opportunities of mixing and splitting among recycle streams, feed streams and entrainer streams. These streams are first split into several sub-streams when flowing into the DN. These splitters are indicated using a set SP, which is the subset of $UNIT$. The sub-streams are then sent into mixers to mix with one another to generate proper feed streams for the distillation columns. These mixers are indicated using a set MX, also the subset of $UNIT$. When flowing out of the DN, the mixtures are split into its different separation sequences. These mass balance constraints are written as follows:

$$f_{sp}^{\text{in}} = \sum_{mx \in MX} fs_{sp,mx} \quad \forall sp \in SP \tag{12}$$

$$f_{mx}^{\text{out}} = \sum_{sp \in SP} fs_{sp,mx} \quad \forall mx \in MX \tag{13}$$

$$f_{mx}^{\text{out}} \cdot \boldsymbol{c}_{mx}^{\text{out}} = \sum_{sp \in SP} fs_{sp,mx} \cdot \boldsymbol{c}_{sp}^{\text{in}} \quad \forall mx \in MX \tag{14}$$

where $fs_{sp,mx}$ denotes the flowrate out of splitter sp to mixer mx. Note that equation (14) is bilinear.

Since output streams of mixer mx and input streams of splitter sp are corresponding

to column feeds and products, respectively, $\boldsymbol{c}_{mx}^{\text{out}}$ and $\boldsymbol{c}_{sp}^{\text{in}}$ are restricted in some regions of the composition space. More specifically, as the potential column feed, $\boldsymbol{c}_{mx}^{\text{out}}$ will be located in some regions identified by algorithms 1 and 2, while the column product $\boldsymbol{c}_{sp}^{\text{in}}$ will be located in the boundary surface of the corresponding region. These stream location constraints are represented using the following equations:

$$\boldsymbol{n}_{bs_{mx}} \cdot \left(\hat{\boldsymbol{c}}_{mx}^{out} - \boldsymbol{s}_{bs_{mx}} \right) \left[\leq, =, \geq \right] 0 \quad \forall mx \in MX,\ bs_{mx} \in BS_{MX} \qquad (15)$$

$$\boldsymbol{n}_{bs_{sp}} \cdot \left(\hat{\boldsymbol{c}}_{sp}^{in} - \boldsymbol{s}_{bs_{sp}} \right) \left[\leq, =, \geq \right] 0 \quad \forall sp \in SP,\ bs_{sp} \in BS_{SP} \qquad (16)$$

where the vector $\boldsymbol{n}_{bs_{mx}}$ or $\boldsymbol{n}_{bs_{sp}}$ denotes the normal vector of the corresponding boundary surface of mixer mx output or splitter sp input; the vector $\boldsymbol{s}_{bs_{mx}}$ or $\boldsymbol{s}_{bs_{sp}}$ denotes the composition vector of any singular point in the corresponding boundary surface; $\left[\leq, =, \geq \right]$ stands for less than, more than or equal, which is determined by substituting a certain composition vector in the corresponding region into the above equations.

OP-RCM

With algorithm 4, the candidate operations are generated, i.e., a series of azeotropic distillation columns. The action of OP-RCM is to organize these operations in a convenient and efficient way. In this article, we use a forest structure composed of a set of binary trees to represent it. Every binary tree corresponds to a simple column sequence, which we call an azeotropic distillation tree. The depth of each binary tree is for optimization, so a hierarchy representation of these binary trees is proposed. Each binary tree is divided into several stages, with each stage corresponding to a simple

column. Hence, the number of stages depends on the maximum depth of each separation tree. Each stage of a binary tree has one feed $f^{in}_{adtr,k_{adtr}}$ and two products, $f^{out1}_{adtr,k_{adtr}}$ and $f^{out2}_{adtr,k_{adtr}}$. $f^{out1}_{adtr,k_{adtr}}$ stands for the flowrate of the pure component stream, while $f^{out2}_{adtr,k_{adtr}}$ stands for the flowrate of the impure stream containing azeotropes. $f^{out1}_{adtr,k_{adtr}}$ flows out of OP-RCM as a final product, while $f^{out2}_{adtr,k_{adtr}}$ is split into two sub-streams with one flowing into the next stage for further separation and the other flowing out of OP-RCM into other blocks, i.e., DN or OP-AO. The mass balance around each azeotropic distillation column is written as:

$$f^{in}_{adtr,k_{adtr}} = f^{out1}_{adtr,k_{adtr}} + f^{out2}_{adtr,k_{adtr}} \quad \forall adtr \in ADTR, k_{adtr} \in K_{ADTR} \tag{17}$$

$$f^{in}_{adtr,k_{adtr}} \cdot \boldsymbol{c}^{in}_{adtr,k_{adtr}} = f^{out1}_{adtr,k_{adtr}} \cdot \boldsymbol{c}^{in}_{adtr,k_{adtr}} + f^{out2}_{adtr,k_{adtr}} \cdot \boldsymbol{c}^{in}_{adtr,k_{adtr}} \quad \forall adtr \in ADTR,\ k_{adtr} \in K_{ADTR} \tag{18}$$

$$f^{in}_{adtr_{mx},1} = f^{out}_{mx} \quad \forall adtr_{mx} \in ADTR_{MX},\ mx \in MX \tag{19}$$

$$\boldsymbol{c}^{in}_{adtr,1_{adtr}} = \boldsymbol{c}^{out}_{mx} \quad \forall adtr_{mx} \in ADTR_{MX},\ mx \in MX \tag{20}$$

$$f^{out2}_{adtr,k_{adtr}} = f^{in}_{adtr,(k+1)_{adtr}} + f^{in}_{sp_{adtr,k_{adtr}}} \quad \forall adtr \in ADTR, k_{adtr} \in K_{ADTR} \tag{21}$$

$$\boldsymbol{c}^{in}_{sp_{adtr,k_{adtr}}} = \boldsymbol{c}^{out2}_{adtr,k_{adtr}} \tag{22}$$

where $ADTR$ denotes the set of azeotropic distillation trees; K_{ADTR} denotes the stages of $adtr$; $(ADTR, K_{ADTR})$, a subset of $UNIT$, denotes the column in stage k of $adtr$; $ADTR_{MX}$ denotes the corresponding $adtr$ of mixer mx; $sp_{adtr,k_{adtr}}$ denotes the corresponding splitter sp of column $(adtr, k_{adtr})$.

The modified Fenske-Underwood-Gilliland (FUG) method proposed by Liu et al.[27] is adopted to predict the design performance of the columns. To use the FUG method for shortcut design of azeotropic distillation columns, the natural composition vector has to be transformed into an expanded composition vector in terms of all singular points.

For instance, the natural composition vector of the column feed stream is represented as:

$$\boldsymbol{c}^{in}_{adtr,k_{adtr}} = \left(c^{in,1}_{adtr,k_{adtr}}, c^{in,2}_{adtr,k_{adtr}}, \cdots, c^{in,i}_{adtr,k_{adtr}}, \cdots, c^{in,M}_{adtr,k_{adtr}}\right)^T \quad (23)$$

where M is the number of components.

Its expanded composition vector is written as:

$$\tilde{\boldsymbol{c}}^{in}_{adtr,k_{adtr}} = \left(\tilde{c}^{in,1}_{adtr,k_{adtr}}, \tilde{c}^{in,2}_{adtr,k_{adtr}}, \cdots, \tilde{c}^{in,j}_{adtr,k_{adtr}}, \cdots, \tilde{c}^{in,N}_{adtr,k_{adtr}}\right)^T \quad (24)$$

where N is the number of singular points. If the number of azeotropes is A, then $N = M + A$.

The transformation is performed using a transformation matrix T:

$$\boldsymbol{T}\left(C^i_j\right) = \begin{bmatrix} C^1_1 & C^1_2 & \cdots & C^1_j & \cdots & C^1_N \\ C^2_1 & C^2_2 & \cdots & C^2_j & \cdots & C^2_N \\ \vdots & \vdots & \vdots & \vdots & \vdots & \vdots \\ C^i_1 & C^i_2 & \cdots & C^i_j & \cdots & C^i_N \\ \vdots & \vdots & \vdots & \vdots & \vdots & \vdots \\ C^M_1 & C^M_2 & \cdots & C^M_j & \cdots & C^M_N \end{bmatrix} \quad (25)$$

$$\boldsymbol{T}\tilde{\boldsymbol{c}} = \boldsymbol{c} \quad (26)$$

where each column of T refers to an azeotrope, and each column vector represents the azeotrope's composition.

With the transformed composition vector, the FUG method is then used:

$$Nmin_{adtr,k_{adtr}} = \frac{\log\left[\left(\frac{\tilde{c}^{D,LK}_{adtr,k_{adr}}}{\tilde{c}^{D,HK}_{adtr,k_{adr}}}\right) \Big/ \left(\frac{\tilde{c}^{B,LK}_{adtr,k_{adr}}}{\tilde{c}^{B,HK}_{adtr,k_{adr}}}\right)\right]}{\log \alpha^{\mathrm{LK,HK}}_{adtr,k_{adtr}}} \quad \forall adtr \in ADTR,\ k_{adtr} \in K_{ADTR} \quad (27)$$

$$\tilde{\boldsymbol{c}}^{D}_{adtr,k_{adtr}} = \tilde{\boldsymbol{c}}^{out1}_{adtr,k_{adtr}},\ \tilde{\boldsymbol{c}}^{B}_{adtr,k_{adtr}} = \tilde{\boldsymbol{c}}^{out2}_{adtr,k_{adtr}}$$

or

$$\tilde{\boldsymbol{c}}^{D}_{adtr,k_{adtr}} = \tilde{\boldsymbol{c}}^{out2}_{adtr,k_{adtr}},\ \tilde{\boldsymbol{c}}^{B}_{adtr,k_{adtr}} = \tilde{\boldsymbol{c}}^{out1}_{adtr,k_{adtr}} \quad (28)$$

$$1-q=\sum_{j}\frac{\alpha_j\tilde{c}^{in,j}_{adtr,k_{adtr}}}{\alpha_j-\theta_{adtr,k_{adtr}}}\quad \forall adtr\in ADTR,\ k_{adtr}\in K_{ADTR} \tag{29}$$

$$Rmin_{adtr,k_{adtr}}+1=\sum_{j}\frac{\alpha_j\tilde{c}^{D,j}_{adtr,k_{adtr}}}{\alpha_j-\theta_{adtr,k_{adtr}}}\quad \forall adtr\in ADTR,\ k_{adtr}\in K_{ADTR} \tag{30}$$

$$R_{adtr,k_{adtr}}=kr_{adtr,k_{adtr}}\,Rmin_{adtr,k_{adtr}}\quad \forall adtr\in ADTR,\ k_{adtr}\in K_{ADTR} \tag{31}$$

$$\frac{N_{adtr,k_{adtr}}-Nmin_{adtr,k_{adtr}}}{N_{adtr,k_{adtr}}+1}=0.75\left[1-\left(\frac{R_{adtr,k_{adtr}}-Rmin_{adtr,k_{adtr}}}{R_{adtr,k_{adtr}}+1}\right)^{0.566}\right]\quad \forall adtr\in ADTR,\ k_{adtr}\in K_{ADTR} \tag{32}$$

where $\tilde{\boldsymbol{c}}^{D}_{adtr,k_{adtr}}$ and $\tilde{\boldsymbol{c}}^{B}_{adtr,k_{adtr}}$ are the expanded composition vectors of the distillate and bottom streams, respectively; $\alpha^{\mathrm{LK,HK}}_{adtr,k_{adtr}}$ denotes the relative volatility between the light key and the heavy key of column $(adtr,k_{adtr})$; $\theta_{adtr,k_{adtr}}$ is the common root of Underwood equation of column $(adtr,k_{adtr})$; $Nmin_{adtr,k_{adtr}}$, $N_{adtr,k_{adtr}}$, $Rmin_{adtr,k_{adtr}}$ and $R_{adtr,k_{adtr}}$ are the minimum number of stages, number of stage, minimum reflux ratio, and reflux ratio of columns $(adtr,k_{adtr})$, respectively; $kr_{adtr,k_{adtr}}$ is the reflux ratio coefficient, it's value is between 1.2 and 2.

Liu et al.[27] mentioned that the relative volatility between singular points is derived in the following way: first choose a point in a compartment and calculate its equilibrium gas phase composition, then represent both the liquid and gas phase composition in terms of singular points, and finally, calculate the relative volatility between the compartment's vertex point according to its definition. In each compartment, the equilibrium of a set of points with uniform distribution as the liquid composition is calculated with the Aspen Plus process simulator. However, many pairs locate in different compartments, which make the results meaningless, which is due to the curvature of the distillation boundaries and fuzziness of compartment boundaries.

Vogelpohl[25] suggested that the relative volatilities between a binary azeotrope and its two pure components are calculated as follows:

$$\alpha_{i,k} = \frac{\gamma_i p_i^s}{\gamma_k p_k^s}$$

where γ_i and γ_k are the s calculated by the chosen VLE model; p_i^s and p_i^s are the saturated pressure calculated by Antoine Equation. For a pure component, its activity coefficient is set to 1. For an azeotrope, the product $\gamma_{az} p_{az}^s$ is defined as follows:

$$\gamma_{az} p_{az}^s = \gamma_A p_A^s = \gamma_B p_B^s = p_{az}$$

where A and B are the two pure components of the azeotrope.

When a ternary or quaternary azeotrope is present in the system, the corresponding relative volatilities are defined as the initial slope of $\boldsymbol{y}^* / \boldsymbol{x}$ along the distillation boundaries. This is a generalization of the following fact: in a binary system, the $\boldsymbol{y}^* / \boldsymbol{x}$ curve is written as follows:

$$y^* = \frac{\alpha x}{1+(\alpha-1)x}$$

and the initial slope equals the relative volatility α. Compared with simulation results, Vogelpohl's method is more accurate and is therefore used in this article.

Finally as shown by several simulation results, assume constant molar flow inside the columns, and that the feed streams of the columns are saturated liquid, i.e., $q=1$. Consequently, the condenser duty and the reboiler duty are calculated as follows:

$$Q^C_{adtr,k_{adtr}} = \overline{r}^C_{adtr,k_{adtr}} f^D_{adtr,k_{adtr}} \left(R_{adtr,k_{adtr}} + 1\right) \qquad \forall adtr \in ADTR,\ k_{adtr} \in K_{ADTR} \tag{33}$$

$$Q^R_{adtr,k_{adtr}} = \overline{r}^R_{adtr,k_{adtr}} f^D_{adtr,k_{adtr}} \left(R_{adtr,k_{adtr}} + 1\right) \qquad \forall adtr \in ADTR,\ k_{adtr} \in K_{ADTR} \tag{34}$$

where $\bar{r}^{C}_{adtr,k_{adtr}}$ and $\bar{r}^{R}_{adtr,k_{adtr}}$ are the average latent heat of distillate and bottom stream of column $(adtr, k_{adtr})$, respectively.

OP-AO

In the OP-AO block, auxiliary methods are embedded. According to the selected auxiliary method, OP-AO has different representations. Here two options for decanting and extractive distillation are introduced.

OP-AO with decanting

When there is a liquid-liquid envelope in the system and decanting is involved in OP-AO for dealing with unchangeable points, the mixer output streams located in the heterogeneous regions are split into the corresponding azeotropic distillation tree and potential decanting operation:

$$f^{out}_{mx} = f^{in}_{adtr_{mx},1} + f^{in}_{dec_{mx}} \quad \forall mx \in MX \tag{35}$$

where $f^{in}_{dec_{mx}}$ denotes input stream of the corresponding decanter of the mixer mx.

The mass balance constraints are written as follows:

$$f^{in}_{dec} = f^{out1}_{dec} + f^{out2}_{dec} \quad \forall dec \in DEC \tag{36}$$

$$f^{in}_{dec} \cdot \boldsymbol{c}^{in}_{dec} = f^{out1}_{dec} \cdot \boldsymbol{c}^{out1}_{dec} + f^{out2}_{dec} \cdot \boldsymbol{c}^{out2}_{dec} \quad \forall dec \in DEC \tag{37}$$

OP-AO with extractive distillation

When using extractive distillation for facilitating further separation of unchangeable points, the output streams of OP-RCM located at unchangeable point are sent to OP-PO. The model of extractive distillation column also uses the FUG method.

However, since the extractive distillation column has two feeds, it has to be mapped into a simple column for detailed design. The feed of the mapped simple column is the stream located at the unchangeable point, and the products are the two corresponding pure species, with the relative volatility between the light key and heavy key in extractive distillation columns relevant to the flowrate of the entrainer and the reflux ratio. On the basis that the relative volatility increases with the entrainer's concentration, we simply assume that the relative volatility is proportional to the composition of entrainer in the liquid phase:

$$\alpha_{ed}^{LK,HK} = \alpha_{ed}^{0} \frac{fe_{ed}}{fe_{ed} + R_{ed} f_{ed}^{D}} + 1 \quad \forall ed \in ED \quad (38)$$

where ED is the set of extractive distillation columns; α_{ed}^{0} is the proportionality coefficient; fe_{ed} is the feed entrainer flowrate. When there is no entrainer feed, the relative volatility is 1, and hence the stream located at the unchangeable point is not able to be separated. While with a constant entrainer feed, the relative volatility is more than 1, it decreases when the reflux ratio increases, since the entrainer is diluted by the reflux.

On the other hand, from the Underwood equation, with a sharp separation of the unchangeable point stream, the relation between the minimum reflux ratio and the relative volatility is derived as follows:

$$Rmin_{ed} = \frac{1}{c_{ed}^{in,LK}\left(\alpha_{ed}^{LK,HK} - 1\right)} \quad \forall ed \in ED \quad (39)$$

Equation 38 and 39 indicate that there is a linear relation between the reflux ratio and the minimum reflux ratio:

$$R_{ed} = \frac{\alpha_{ed}^{0} c_{ed}^{in,LK} fe_{ed}}{f_{ed}^{D}} Rmin_{ed} - \frac{fe_{ed}}{f_{ed}^{D}} \quad \forall ed \in ED \quad (40)$$

Naturally, the reflux ratio has to be greater than the minimum reflux ratio. Let $R_{ed} \geq Rmin_{ed}$, the minimum entrainer flowrate is then as follows:

$$fe_{ed}^{\min} = \frac{f_{ed}^{D}}{\alpha_{ed}^{0} c_{ed}^{in,LK}} \quad \forall ed \in ED \quad (41)$$

In this way, the same FUG method is used as mentioned before.

Objective Function

The total annualized cost (TAC) is used in this article as the objective function, including column cost and utility cost:

$$TAC = \sum_{col \in COL} y_{col} \left(\mathrm{K} N_{col} + \mathrm{B} \right) + \sum_{col \in COL} \left(\mathrm{P}_h Q_{adtr,k_{adtr}}^{R} + \mathrm{P}_c Q_{adtr,k_{adtr}}^{C} \right) \quad (42)$$
$$COL = (ADTR, K_{ADTR}) \bigcup ED$$

where y_{col} denotes the existence of the column col; N_{col} denotes the number of stages of the column col; the set COL denotes all columns in the flowsheet; K, B, P_h and P_c are relevant annualized cost coefficients.

Solution Strategy

Finally, the overall synthesis problem is formulated as an MINLP model. In this article, the model is solved using the DICOPT[28] solver in GAMS environment, with CONOPT and CPLEX embedded for NLP and MIP sub-problems respectively. In order to maximizing the likelihood of finding the global optimum solution, several starting points are used in the solution of the example problems. Due to the strong nonlinearity mainly caused by the FUG equations, initial feasible solutions are rather difficult to be

obtained. In this work, a two-stage solution strategy is proposed to improve the efficiency of solving the model. In the first stage, a reduced NLP model without detailed column design is solved by minimizing the random total column load:

$$\text{random total column load} = \sum_{col \in COL} rand_{COL} \cdot f_{COL}^{in} \quad (44)$$

where $rand_{COL}$ is a set of random weights for each column load. Specially, when $rand_{COL}$ are all set to 1, the objective becomes the total column load. The reduced model only deals with mass balance equations. Its nonlinearity is aroused by the product of the flowrate and the composition of streams. Therefore, it is bilinear and easy to solve. Since the solution satisfies all the mass balance constraints, the corresponding scheme is a feasible one. Apply the modified FUG method to the feasible scheme, its detailed design parameters are easily calculated and consequently a feasible solution for the overall model is obtained. In the second stage, the feasible solution is used as the initial guess, and then solve the original MINLP model using the DICOPT solver. The random weight for each column load ensures that several random starting points are generated for the overall model, which enhances the solution performance to achieve the global optimum solution. The scale of the random weights $rand_{COL}$ affect the random level of the generated starting points for the second stage, which is very important for covering the entire solution space. If the scale of $rand_{COL}$ is too small, the generated starting points probably hit the same one, whereas if the scale of $rand_{COL}$ is too large, the solution in the second stage often lost feasibility. It is found that the scale of $rand_{COL}$ is better to be ten times of the scale of column feeds in the scheme. And in the two example cases, the overall iteration steps are assumed to

be 100.

Illustration and Discussion

In this section, two industrial cases are studied to demonstrate the effectiveness of the proposed framework. One is the ethanol-water-toluene system for the purpose of producing anhydrous ethanol, and the other is the MTBE-methanol-isobutene-butane system for the illustration of mixtures with more than three components.

The ethanol-water-toluene system

The linearized RCMs of ethanol, water and toluene system is shown in Figure 4. The composition space is divided into three distillation regions, which are further divided into two compartments each. Moreover, some compartments are divided into homogeneous and heterogeneous regions by the liquid-liquid envelope. Since an unchangeable point H is identified, decanting is used to facilitate further separation. The superstructure with decanting for this system is shown in Figure 5. There are 900 variables (with 10 binary variables) and 530 constraints in the model, and the average CPU time is 2.55s for the overall model during each iteration.

With a feed of 37.3% ethanol and 62.7% water, the solution of the optimal flowsheet is shown in Figure 6. It is the same as the solution of Feng et al.[21], but since the number of stages and reflux ratio are optimized, about 10% potential reduction of TAC is obtained. This is because in this case the distillate flowrate related to heat duties dominates the overall cost. This flowsheet is similar to the one used in industry (see Figure 7), and in fact identical when columns 1 and 3 in the industrial scheme are

combined into the water column in this flowsheet. As a result, some additional capital cost is saved.

However, the allocation of the feed stream to the ethanol column, the decanter and the water column is sensitive to its composition distribution. As seen in Figure 8, if the feed contains more ethanol, the optimal flowsheet is different and multi-stream mixing and splitting appear. In fact, there are two main approaches to dehydrate the ethanol: one is to remove most of the water in the water column and then use the ternary azeotrope to remove the left; the other is to remove the water totally by the ternary azeotrope. Figure 8 also shows that a diluted feed favors the former one, whereas a concentrated feed favors the latter one. The decanter is capable of adjusting the feed composition and forms hybrid approaches between the two. When the major dehydration method shifts from the former one to the latter one, a peak value of the optimal TAC is present. Table 1 shows the influence of feed allocation on TAC. The inherent reason is that the thermodynamic property of the system renders that the column load dominates the TAC. Since the boiling point of the binary azeotrope X is close to ethanol and consequently their relative volatility is nearly 1, the operation line of the ethanol column usually lies on EH, which makes the number of stages and reflux ratio of the ethanol column changes little. On the other hand, the relative volatility between X and water is large enough, and therefore, the column load has stronger effect on the TAC than the number of stages and reflux ratio. The former dehydration method takes advantage on the total column load with a diluted feed, and it reverses with a concentrated feed.

Next we will show the superstructure in this work is superior to the one proposed by Feng et al.[21] from the two-column flowsheet. One column is for producing pure ethanol, and the other is for producing pure water, with some stream containing toluene recycling in the flowsheet as an entrainer. Assume the operating line of the ethanol column is the one shown in Figure 9, and then the operating line of water column can be located in three regions: compartment 1, homogeneous of compartment 2, or heterogeneous region of compartment 2. Then Q, R, S and P will be where the DN input streams located. With the constraint of mass balance, another flowsheet feasibility test rule is constructed:

Flowsheet feasibility test rule 2

The feed to the columns has to lie in the convex polygon area bounded by the lines between the DN input streams.

So Figure 9(a) is infeasible, while Figures 9(b) and 9(c) are feasible. For the model of Feng et al.[21], the feasible area with only two-stream mixing is the skeleton according to the lines between the DN input streams. However, for the model of ours, the feasible area with multi-stream mixing and stream splitting is the whole convex area bounded by the lines between the DN input streams as seen in Figure 10. Hence, the multi-stream mixing and the stream splitting significantly enlarge the feasible area.

In addition, due to the lack of multi-stream mixing, the model of Feng et al.[21] fails to deal with point 4 in an alternative two-column flowsheet (see Figure 11), and therefore

it will significantly reduce the recovery level. If the lines between a point and the other DN input stream points intersect no operation lines after removing the self-loop, we call these *isolated points*. The flowsheet feasibility test rule 3 is then stated as follows:

Flowsheet feasibility test rule 3

Isolated points are only dealt with multi-stream mixing.

For the above two reasons, multi-stream mixing and stream splitting significantly improve the recovery rate.

The MTBE-methanol-isobutene-butane system

The linearized RCMs of MTBE, methanol, isobutene and butane are shown in Figure 12. Two distillation regions Z-Y-X-Methanol and Z-Isobutene-Y-Butane-X-MTBE are identified by the system analysis, and the latter distillation region is further divided into three compartments Z-Y-X-MTBE, Z-Y-Butane-MTBE and Z-Isobutene-Butane-MTBE. An unchangeable point Z is identified. Since it is a homogeneous system, we use extractive distillation with water as an entrainer to facilitate the separation. The superstructure with extractive distillation for this system is shown in Figure 13. There are 1099 variables (with 51 binary variables) and 840 constraints in the model, and the average CPU time is 5.72s for the overall model during each iteration.

The optimal design with a feed of 4.5% isobutene, 8.5% butane, 75% methanol and

12% MTBE is shown in Figure 14. The feed first removes methanol and leaves a mixture located on distillation boundary XYZ. With the help of mixing with isobutene, MTBE and butane in the mixture are released, and changeable points X and Y are transformed into unchangeable point Z. For a minimum flowrate of isobutene, the mixer output stream is exactly located on the compartment boundary ZBM. Then the stream located at the unchangeable point Z is separated using extractive distillation. This flowsheet is used for illustrating the effectiveness of the proposed framework, since the system is treated as a non-reacting system and the unchangeable point Z is broken by extractive distillation. Compared with this scheme, Z is broken by the reaction of isobutene and methanol which yields MTBE in an industrial scheme. To optimize such systems, a reaction block in the OP-AO is required, which will be considered in our future work.

Conclusion

In this work, a systematic and efficient methodology has been proposed for synthesizing the optimal separation process of azeotropic mixtures. Compared with current methods, the present method is believed to be superior in the following aspects. First, the superstructure allows the flowsheet to be more flexible and efficient. Mixing provides more degrees of freedom for crossing the distillation boundaries, and the splitting allows a process stream to be sent into different operation units for a higher efficiency. Based on the above facts, some rules were proposed for the feasibility test of recycle streams. Second, the system analysis is well suited for large numbers of components involved in the system. Since it is quite difficult to obtain perfect recovery

process using only distillation and mixing, especially for a homogeneous system, detection of unchangeable points before the optimization determines the recovery limitation of specific component and suggests the use of other technologies such as pressure swing distillation and extractive distillation. Third, A TAC (Total Annualized Cost) objective function has been proposed for assessing the cost of practical processes by detailed design parameters (i.e., stage number, reflux ratio). The TAC accounts for the number of stages and the reflux ratio calculated by a shortcut method.

Acknowledgment

The authors in Dalian University of Technology would like to acknowledge the financial support provided by the National Natural Science Foundation of China, under Grant No. 20876020, and the support of Center for Advanced Process Decision-making (CAPD) in Carnegie Mellon University. Prof. Alfons Vogelpohl at Clausthal University of Technology in Germany is gratefully acknowledged for providing the detailed information about how to calculate the relative volatilities between azeotropes and other singular points.

Literature Cited

1. Doherty J. On the dynamics of distillation processes--III: The topological structure of ternary residue curve maps. *Chemical Engineering Science.* 1979; **34**(12): 1401-1414.

2. Safrit B, Westerberg A. Algorithm for generating the distillation regions for azeotropic multicomponent mixtures. *Industrial & Engineering Chemistry Research.* 1997; **36**(5): 1827-1840.

3. Thong D, Jobson M. Multicomponent homogeneous azeotropic distillation 1. Assessing product feasibility. *Chemical Engineering Science.* 2001; **56**(14): 4369-4391.

4. Fien G, Liu Y. Heuristic synthesis and shortcut design of separation processes using residue curve maps: a review. *Industrial & Engineering Chemistry Research.* 1994; **33**(11): 2505-2522.

5. Widagdo S, Seider W. Journal review: Azeotropic distillation. *AIChE Journal.* 1996; **42**(1): 96-130.

6. Fidkowski Z, Malone M, Doherty M. Computing azeotropes in multicomponent mixtures. *Computers & Chemical Engineering.* 1993; **17**(12): 1141-1155.

7. Rooks R, Julka V, Doherty M, Malone M. Structure of distillation regions for muiticomponent azeotropic mixtures. *AIChE Journal.* 1998; **44**(6): 1382-1391.

8. Doherty M, Caldarola G. Design and synthesis of homogeneous azeotropic distillations. 3. The sequencing of columns for azeotropic and extractive distillations. *Industrial & Engineering Chemistry Fundamentals.* 1985; **24**(4): 474-485.

9. Pham H, Doherty M. Design and synthesis of heterogeneous azeotropic distillations--III. Column sequences. *Chemical Engineering Science.* 1990; **45**(7): 1845-1854.

10. Safrit B, Westerberg A. Synthesis of azeotropic batch distillation separation systems. *Industrial & Engineering Chemistry Research.* 1997; **36**(5): 1841-1854.

11. Thong D, Jobson M. Multicomponent homogeneous azeotropic distillation 3. Column sequence synthesis synthesis. *Chemical Engineering Science.* 2001; **56**(14): 4417-4432.

12. Thong D, Liu G, Jobson M, Smith R. Synthesis of distillation sequences for separating multicomponent azeotropic mixtures. *Chemical Engineering and*

Processing. 2004; **43**(3): 239-250.

13. Tao L, Malone M, Doherty M. Synthesis of azeotropic distillation systems with recycles. *Industrial & Engineering Chemistry Research.* 2003; **42**(8): 1783-1794.

14. Liu G, Jobson M, Smith R, Wahnschafft O. Recycle selection for homogeneous azeotropic distillation sequences. *Industrial & Engineering Chemistry Research.* 2005; **44**(13): 4641-4655.

15. Bauer M, Stichlmair J. Superstructures for the mixed integer optimization of nonideal and azeotropic distillation processes. *Computers & Chemical Engineering.* 1996; **20**: S25-S30.

16. Frey T, Bauer M, Stichlmair J. MINLP-optimization of complex column configurations for azeotropic mixtures. *Computers & Chemical Engineering.* 1997; **21**: S217-S222.

17. Bauer M, Stichlmair J. Design and economic optimization of azeotropic distillation processes using mixed-integer nonlinear programming. *Computers and Chemical Engineering.* 1998; **22**(9): 1271-1286.

18. Ismail S, Pistikopoulos E, Papalexandri K. Modular representation synthesis framework for homogeneous azeotropic separation. *AIChE Journal.* 1999; **45**(8): 1701-1720.

19. Yeomans H, Grossmann I. Optimal design of complex distillation columns using rigorous tray-by-tray disjunctive programming models. *Industrial & Engineering Chemistry Research.* 2000; **39**(11): 4326-4335.

20. Sargent R. A functional approach to process synthesis and its application to distillation systems. *Computers & Chemical Engineering.* 1998; **22**(1-2): 31-45.

21. Feng G, Fan L, Seib P, Bertok B, Kalotai L, Friedler F. Graph-theoretic method for the algorithmic synthesis of azeotropic-distillation systems. *Industrial & Engineering Chemistry Research.* 2003; **42**(15): 3602-3611.

22. Feng G, Fan L, Friedler F, Seibs P. Identifying operating units for the design and synthesis of azeotropic-distillation systems. *Industrial & Engineering Chemistry Research.* 2000; **39**(1): 175-184.

23. Bagajewicz M, Manousiouthakis V. Mass/heat-exchange network representation of distillation networks. *AIChE Journal.* 1992; **38**(11): 1769-1800.

24. Bagajewicz M, Pham R, Manousiouthakis V. On the state space approach to

mass/heat exchanger network design. *Chemical Engineering Science.* 1998; **53**(14): 2595-2621.

25. Vogelpohl A. On the relation between ideal and real systems in ternary distillation. *Chemical Engineering Research and Design*. 1999; **77**(6): 487-492.

26. Serafimov L. The azeotropic rule and the classification of multicomponent mixtures VII. Diagrams for ternary mixtures. *Russ. J. Phys. Chem.* 1970; **44**(4): 567–571.

27. Liu G, Jobson M, Smith R, Wahnschafft O. Shortcut design method for columns separating azeotropic mixtures. *Industrial & Engineering Chemistry Research.* 2004; **43**(14): 3908-3923.

28. Viswanathan J, Grossmann I. A combined penalty function and outer-approximation method for MINLP optimization. *Computers & Chemical Engineering.* 1990; **14**(7): 769-782.

Figures

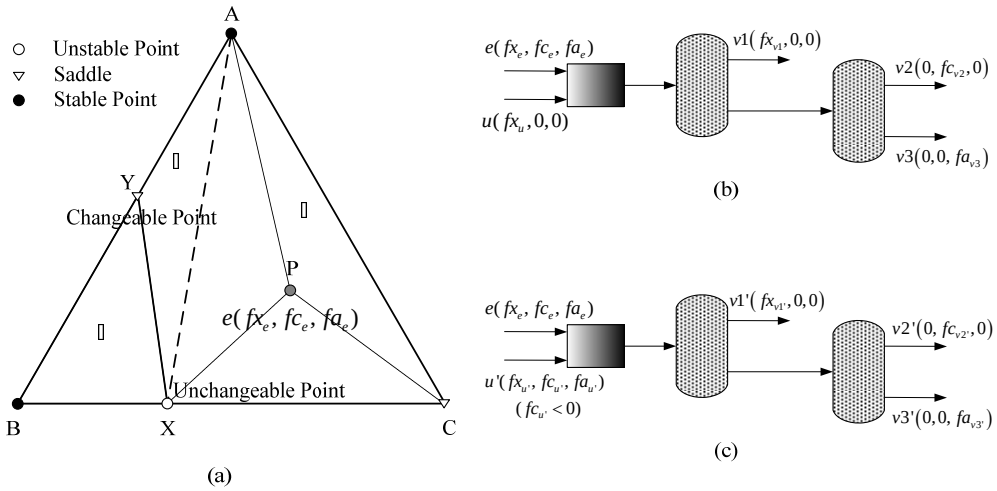

Figure 1. Mixing-distillation pair and unchangeable point

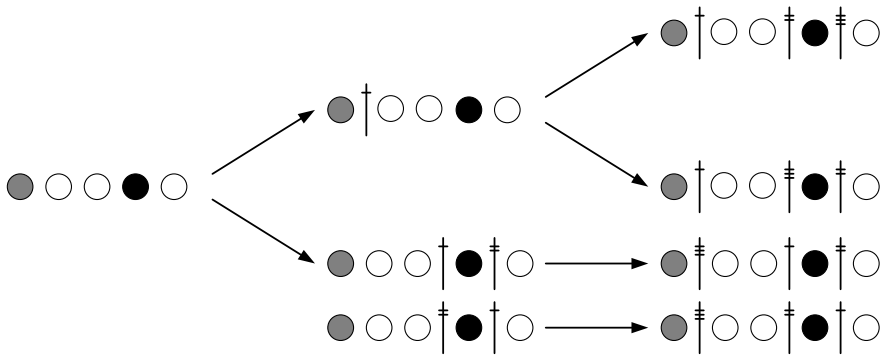

Figure 2. Illustration of Algorithm 4

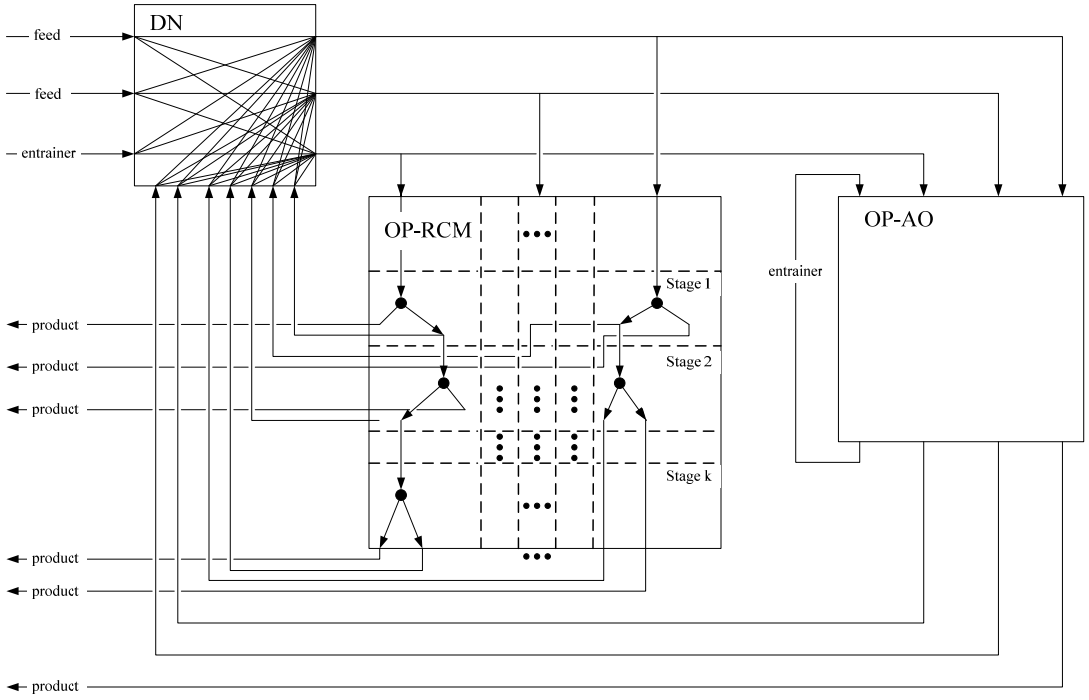

Figure 3. The proposed superstructure

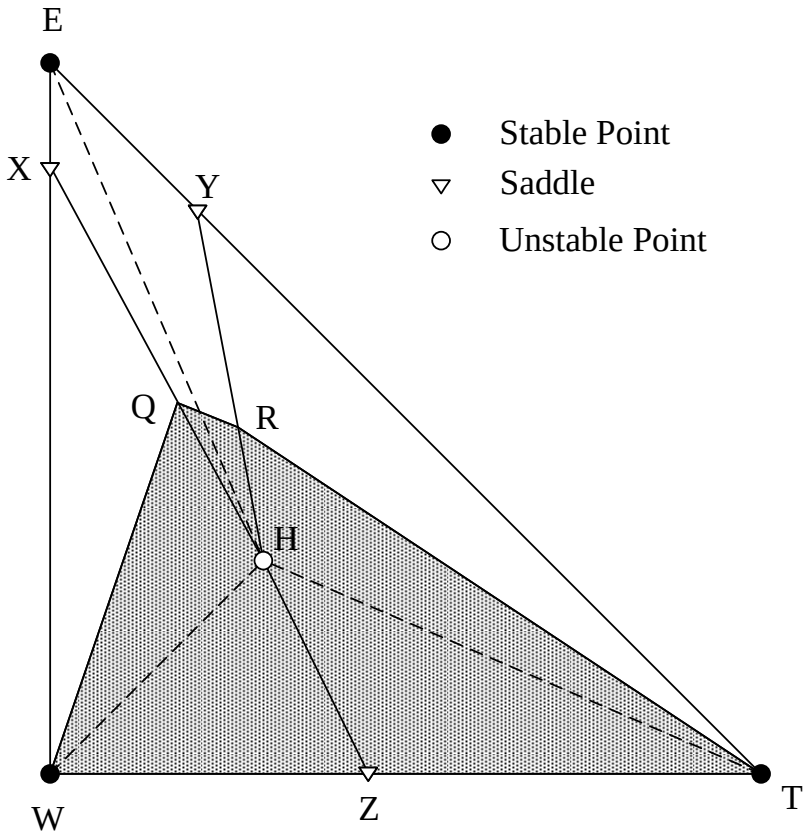

Figure 4. RCMs of the ethanol-water-toluene system

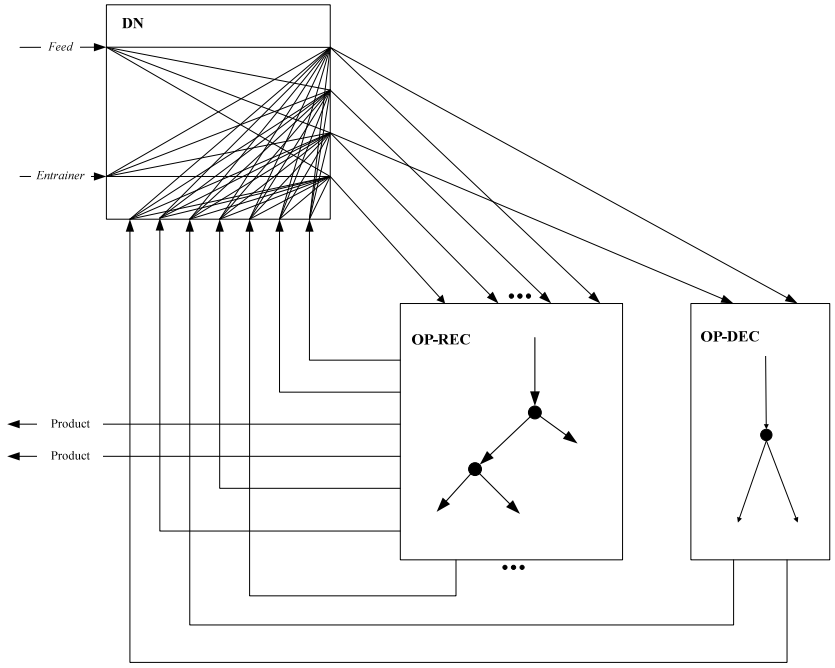

Figure 5. The superstructure with decanting

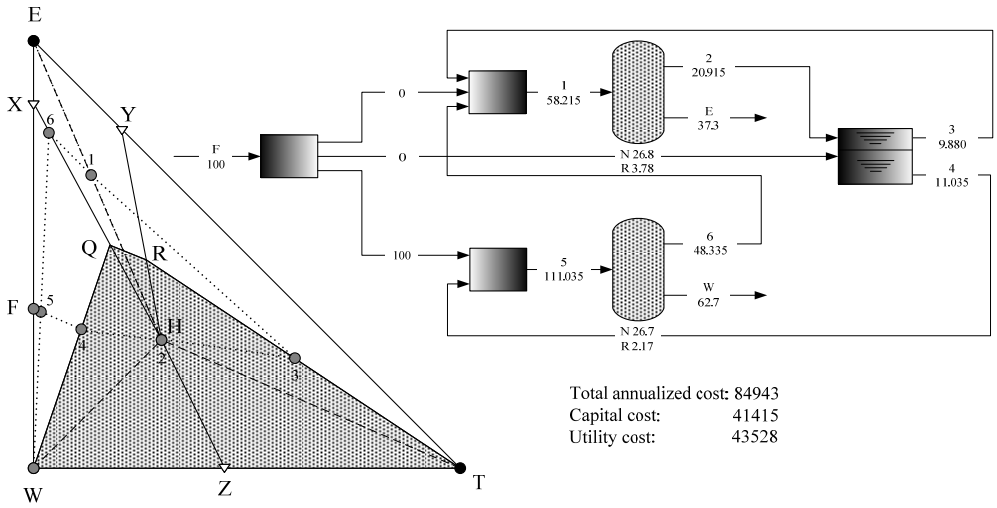

Figure 6. The solution of case 1 with a feed of 37.3% ethanol

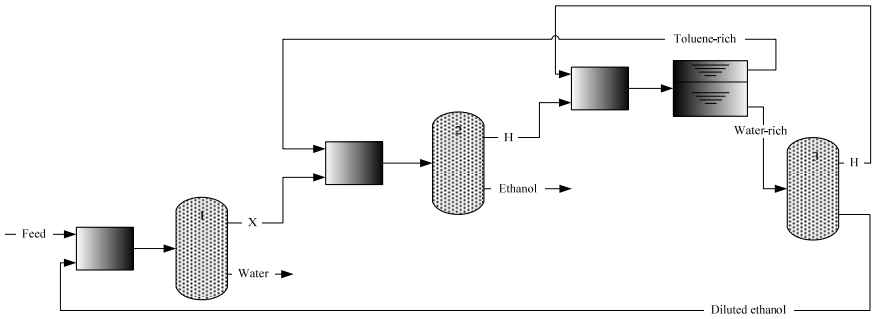

Figure 7. The industrial scheme for producing anhydrous ethanol

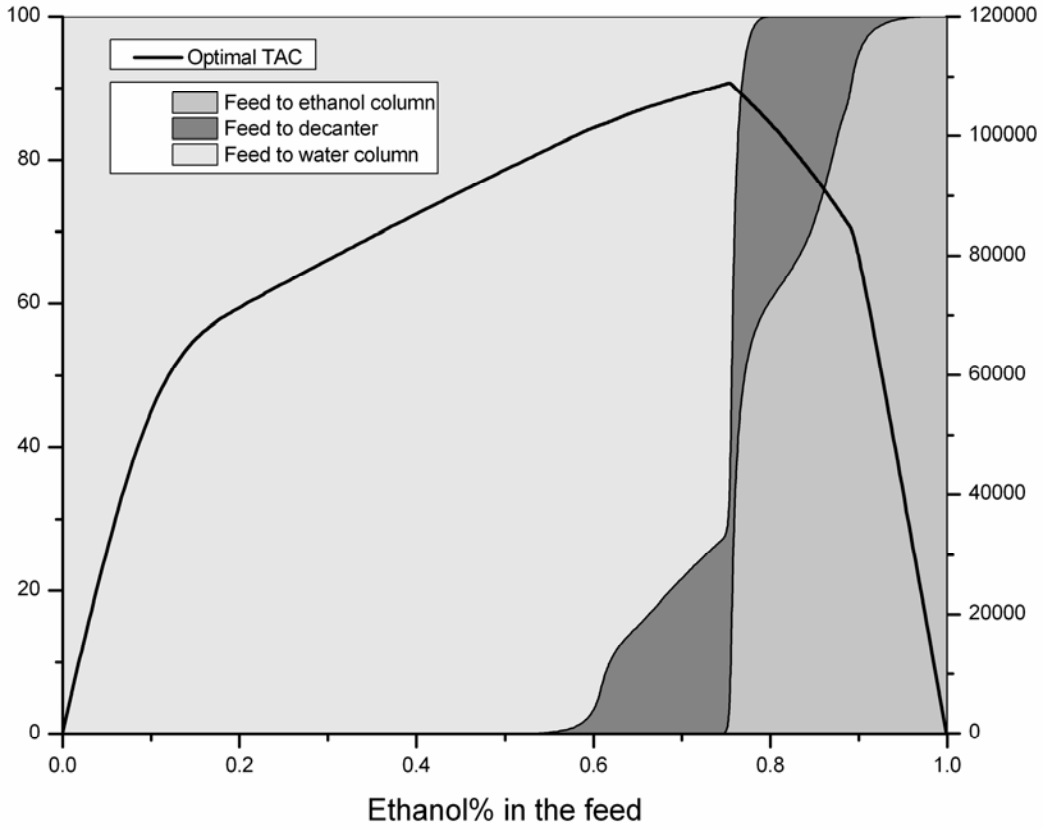

Figure 8. The optimal feed allocation and TAC

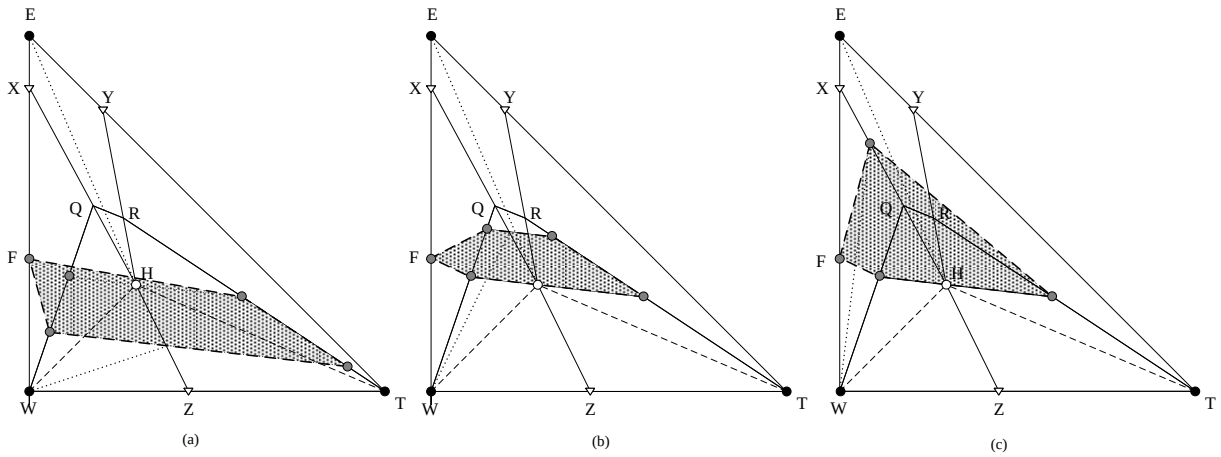

Figure 9. Illustration of rule 2

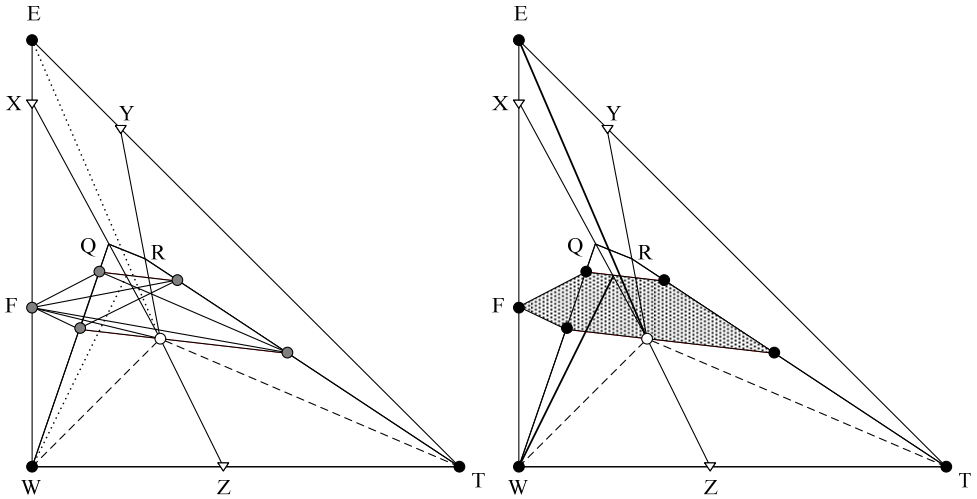

Figure 10. Comparison between models of Feng et al. and ours

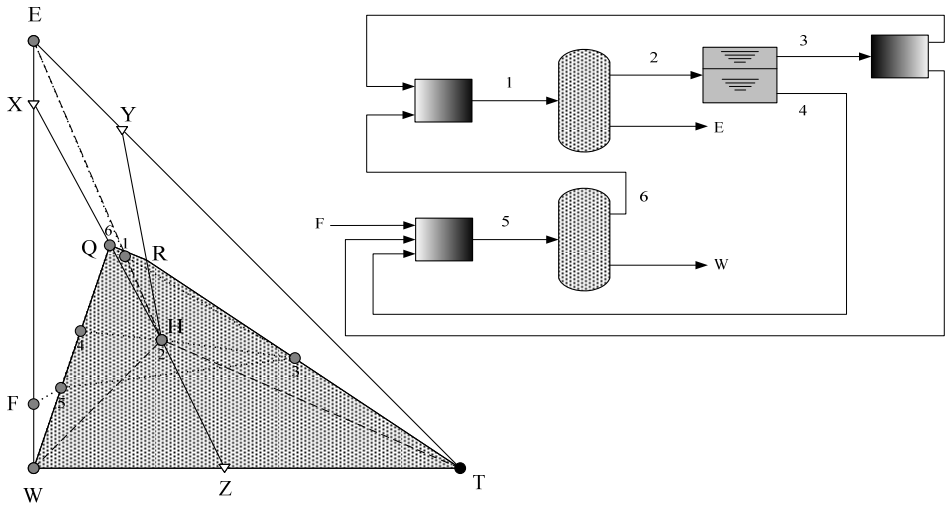

Figure 11. The alternative two-column flowsheet

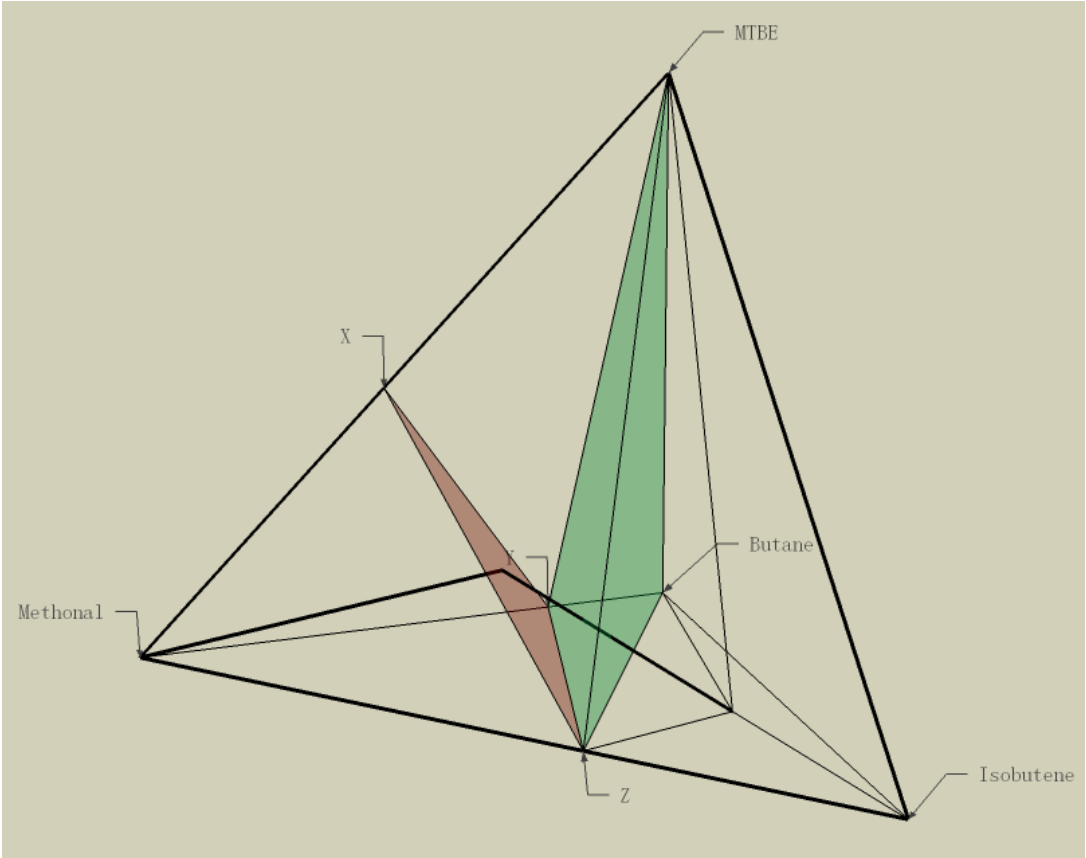

Figure 12. RCMs of the MTBE-methanol-isobutene-butane system

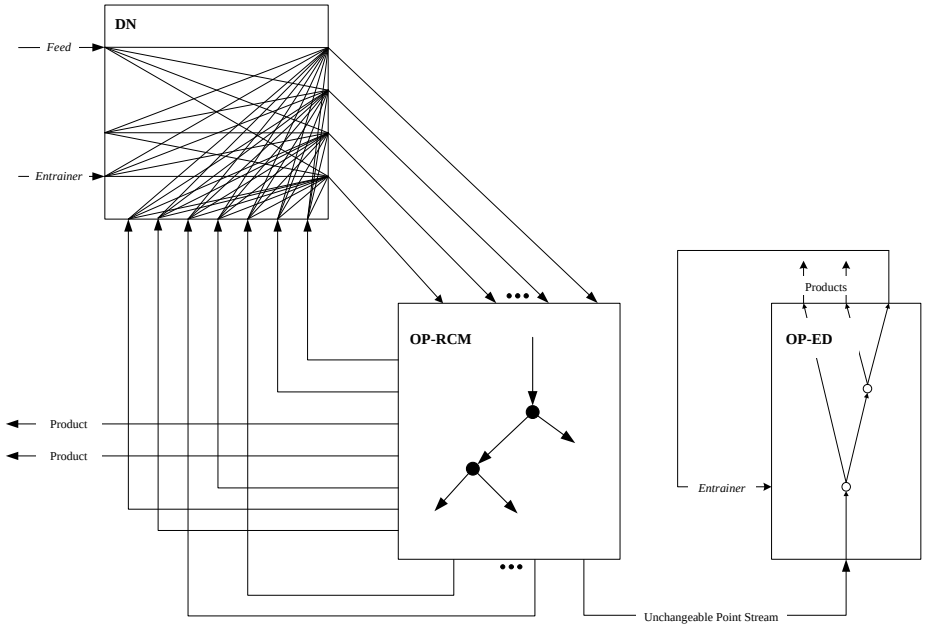

Figure 13. The superstructure with extractive distillation

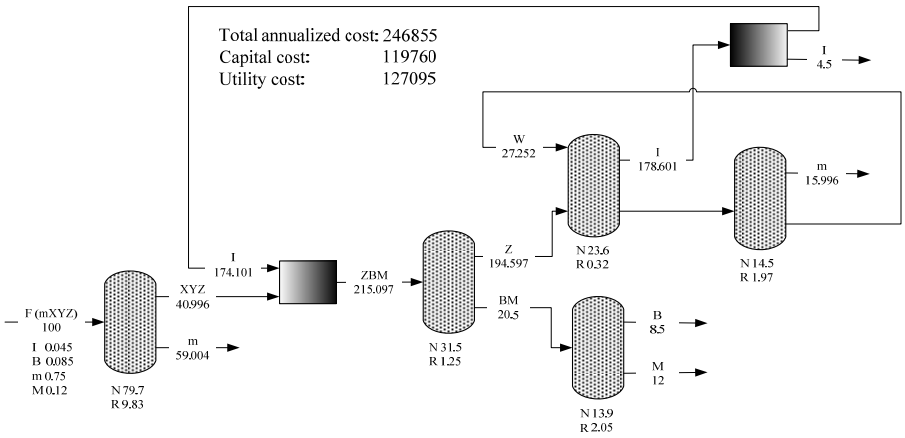

Figure 14. The solution of case 2

Tables

Table 1. Comparison between different feed allocation with a feed of 80% ethanol

Feed allocation	Optimal	Only to water column	Only to ethanol column
Feed to ethanol column	60.963	0	100
Feed to decanter	39.037	0	0
Feed to water column	0	100	0
Ethanol column: number of stages	32.9	31.5	33.0
Ethanol column: reflux ratio	2.369	3.268	2.133
Water column: number of stages	23.2	29.2	22.7
Water column: reflux ratio	1.611	1.107	1.741
Ethanol column load	157.03	124.859	175.796
Water column load	55.159	123.668	50.543
Total load	212.189	248.527	226.339
Capital cost	42852	45359	42635
Utility cost	59638	70216	64831
TAC	102490	115575	107466